Universidad Zaragoza

1542

Departamento de Química Física
Universidad Zaragoza

Facultad de Ciencias
Universidad Zaragoza

Master's Degree on Nanostructured Materials for Nanotechnology Applications

Assembly and characterization of nanostructures for molecular electronic devices

---

Final Master's Project

Author:

Alejandro Gómez González

Supervisors:

Dr. Pilar Cea Mingueza

Dr. Santiago Martín Solans

LMA
LABORATORIO DE MICROSCOPÍAS AVANZADAS

INMA
INSTITUTO DE NANOCIENCIA Y MATERIALES DE ARAGÓN

Zaragoza, 13th June 2023

Title: Assembly and characterization of nanostructures for molecular electronic devices

Author: Alejandro Gómez González

Supervisors: Dr. Pilar Cea Mingueza
Dr. Santiago Martín Solans

Department: Physical Chemistry

Place of realization: Platón research group laboratories, at the Science Faculty and the Institute of Nanoscience and Materials Science, as well as the Laboratory for Advanced Microscopies from the University of Zaragoza

ABSTRACT

Electronic devices have become a central piece of today's society, with an increasing need for getting more powerful, more compact, and importantly, more efficient devices. This can be achieved by reducing the size of each individual component of the device. However, the current technology, CMOS (Complementary Metal-Oxide-Semiconductor), is close to reaching its size limit. Molecular Electronics poses itself as an alternative that would make it possible to continue the current trend of producing more advanced devices. This technology uses a bottom-up approach to produce arrangements of molecules that work as elements of an electronic circuit.

In this Final Master's Project, a compound from the family of the curcuminoids has been studied and characterized both at the air-water interface (Langmuir films) and transferred onto solid supports (Langmuir-Blodgett, LB, and Langmuir-Schaefer, LS, films). The main aim of this work was to fabricate highly ordered monolayers that can act as circuitry elements.

RESUMEN

La sociedad actual demanda dispositivos electrónicos cada vez más eficaces, rápidos, potentes y eficientes. A día de hoy, estos requerimientos se están consiguiendo mediante la reducción paulatina del tamaño de los componentes a través de la tecnología CMOS (del inglés "*Complementary Metal-Oxide-Semiconductor*). Sin embargo, esta tecnología está cerca de alcanzar su límite a la hora de reducir el tamaño de tales elementos. En este contexto la Electrónica Molecular surge como una opción que permitiría continuar con la miniaturización de los componentes de los dispositivos electrónicos. Esta tecnología, a diferencia de CMOS, se basa en un enfoque *bottom-up* para producir estructuras moleculares que funcionan como elementos de un circuito.

En este Trabajo de Fin de Master, un compuesto de la familia de los curcuminoides ha sido estudiado y caracterizado tanto en la interfase aire-agua (monocapa de Langmuir) como transferido sobre sustratos sólidos (películas de Langmuir-Blodgett, LB, y Langmuir-Schaefer, LS). Siendo el objetivo principal de este trabajo la fabricación de monocapas altamente ordenadas del compuesto que puedan actuar como propios elementos del circuito.

TABLE OF CONTENTS

1. INTRODUCTION

1.1 State of the art

It is not possible to imagine today's society without the presence of electronic devices that, in the last few decades, have become a fundamental part of the complex gear system that shapes the world. These electronic devices are indeed governed by a small component, the transistor, which is at the centre of all logical processes that need to take place for such a device to function properly.

By miniaturizing all components in general, but transistors in particular, it is possible to obtain more powerful, more compact and, importantly, more efficient devices. These are the reasons why since the very beginning of the introduction of electronic devices into the market, there has been a growing desire for improving the available technology to, in turn, benefit society as a whole.

Governed by this desire, technology has advanced, and components of electronic devices have become progressively smaller through the years. In fact, back in the year 1965 Gordon E. Moore proposed an empirical law that stated that the number of transistors that fit inside a microprocessor would be doubled every year.[1] Even though 10 years later Moore corrected his prediction based on available data and changed the period to two years instead of one. This law has been valid ever since, but in recent times it has been put in jeopardy due to physical limits inherent to the technology on which transistors are based nowadays.[2]

In the present day, transistors are made by lithography on a monocrystalline silicon wafer, which allows for the preparation of progressively smaller transistors. However, this miniaturization methodology is already reaching its limit due to quantum effects that appear when the size of the features produced is small enough, which results in a loss of the semiconductor properties of silicon. This is why it is not expected for silicon-based transistors to get much smaller in size.[3]

1.2 Molecular electronics

It is therefore necessary to come up with new technologies that can be used to maintain the rate at which the size of transistors has decreased in the last few decades. Molecular electronics is a promising approach with a renaissance in the last few years towards the development of a new electronic technology. [4]

Molecular electronics uses molecules as basic elements in circuitry such as molecular wires, switches, rectifiers, diodes or even transistors. [5] The advantages of using molecules include:

- Size: the molecules have sizes in the order of a few nanometers, and therefore are already in the same size range as the smallest silicon-based transistors. This comes with a set of unique advantages such as faster performance, heightened capacities and high integration density, since many molecules can fit in a single chip and they can even act as individual electric machines.[6]
- Given the quantum nature of charge transport in molecular junctions, Molecular Electronics presents certain unique phenomena.[7]
- The devices formed following the Molecular Electronics principles can be made from a wide range of different molecules that can be synthesised with high purity, resulting in thinner and lighter devices that require lower voltages to operate.[8] Having identical repeating units that form the devices can also lead to lower production costs of the devices.
- By combining organic molecules as electrical components with carbon-based or polymer-based electrodes, can lead to biocompatible devices while also being sustainably fabricated, reducing e-waste and even degrading once the service life of the device has ended.[9,10] These combinations of molecules with organic chemistry-based electrodes can also lead to flexible and transparent devices.
- Lastly, one of the most important and promising properties of Molecular Electronics-based devices is their ability to show thermoelectric behaviour, being capable of using the heat produced by the normal functioning of the device and turn it into usable electricity. This achieves two different objectives: reducing the temperature of the device, thus increasing its service life and protecting its components while also reducing the electronic power needed to run the device.

In terms of device fabrication, one of the main differences between the present CMOS (Complementary Metal-Oxide Semiconductor) technology and molecular electronics is that in this new field, devices are formed in a bottom-up approach, arranging the molecules on top of a substrate in a given pattern, instead of defining features by lithography on a silicon monocrystal.

Nevertheless, the application of Molecular Electronics has encountered several challenging problems that need to be addressed before the technology can be fully implemented in commercial electronic devices.

One of the most important challenges that Molecular Electronics face nowadays is the optimization of interface engineering. Creating a stable, highly conductive and well-defined interface between the electrodes and the molecules is a key requirement for the future obtention of reliable and powerful Molecular Electronics devices.[11]

There are several approaches to improve the interfaces between the molecules and the electrodes: by designing molecules that have anchoring groups with topologies that allow for the proper connection with the substrate, while also having functional groups that enhance the chemical interactions between both components, the properties of the junction would be improved. Another approach to this problem is using multipodal molecules that have more than one anchoring group (bipodal or tripodal), in order to increase the contact stability of the junction.[12]

Another very important challenge that Molecular Electronics faces is the integration of a large number of molecules in an ordered manner without short-circuits and in such a way that all individual elements have the same characteristics. This challenge can be overcome by using preparation techniques that allow for fine control of the deposited molecules, such as Langmuir-Blodgett or Langmuir-Schaefer. [13]

Both techniques are based around the obtention of a monolayer of molecules at the air-liquid interface by compression of superficial barriers that gradually reduce the available area per molecule until the monolayer is completely formed. Once the monolayer has been formed it is possible to put a substrate in contact with the air-liquid interface to transfer the monolayer to the substrate. The transference can be made vertically, by submerging or emerging the substrate from the subphase, so it passes through the molecule monolayer; or horizontally, by putting the substrate in contact with the molecules by suspending it above the interface until contact is made.

These fabrication techniques, that will be explained further in this document, can be used to form 2D molecular arrangements for Molecular Electronics, with very fine control of the coverage.

One especially interesting family of molecules for the preparation of 2D molecular arrangements are Covalent Organic Frameworks (COFs). These are a type of crystalline material formed by organic molecules that are connected by covalent bonds. They are typically formed by light elements such as C, O, H, N and B.[14] Even though COFs can

have a three-dimensional crystalline structure, this work will be based around the obtention of two-dimensional COFs arrangements.

2D-COFs have shown high conductivities when the building blocks present conjugation throughout the whole molecule while also being, in some cases, semiconductors and can therefore show promise for future application in diverse areas such as energy storage, sensing, photodetectors and even electronic devices.[14 15]

These COFs can also be used as molecular scaffolding to further control the position of molecules onto the bottom electrode. This ordering of the molecules makes them behave in a more reproducible way, suppressing cross-talk and in-plane charge transport due to the extra space created between them because of the presence of the scaffold.[16]

In a collaboration with Prof. Nuria Aliaga, from the ICMAB-CSIC of Barcelona, the PLATÓN group has been working on preparing 2D films of molecules capable of forming COFs and studying their properties both at the air-liquid and the air-solid interfaces. One of the most important research lines of FunNanoSurf, the group from Prof. Aliaga, is the optimization of synthesis procedures for the preparation of COFs materials, with a special interest in molecules from the family of curcuminoids.

Curcuminoids are molecules that share the main skeletal structure of curcumin, consisting of two aromatic rings connected by seven conjugated carbon atoms that have two ketone groups at the carbons 3 and 5.

In this project, a molecule from the family of the curcuminoids, compound **1**, has been studied. This molecule shows conjugated double bonds that ensure electronic conductivity in the plane of the molecule and two aromatic rings common to all curcuminoids that allow for π-π interactions that contribute to the organization of the molecules at the air-liquid interface and when transferring them onto substrates.

During this Final Master's Project (FMP), the optimization for the fabrication conditions for Langmuir films, LB and LS, together with the characterization of the molecular electronics properties have been performed as well as some preliminary studies on the electrical properties of the film, that pave the way for further research using this promising material.

2. OBJECTIVES

Academic objectives: one of the most important goals of this Final Master's Thesis is to complete the training of the student. This can be achieved by fulfilling the following objectives:

- To learn to work autonomously as well as to take decisions based on the available information during the development of this research work.
- To learn to work with self-reliance in a nanoscience laboratory following the appropriate guidelines regarding security and rigor.
- To perform literature searches and select the most valuable information from the sources consulted.
- To elaborate this dissertation improving the writing and overall communication skills of the student with its subsequent presentation to the examiners panel.

Didactic objectives: It is expected that the student learns how to work in a nanoscience laboratory and specifics about the characterization techniques.

Scientific objectives:

- The fabrication of highly ordered Langmuir films of a curcumin derivative at the air-water interface.
- The fabrication of Langmuir-Blodgett or Langmuir-Schaefer films with precise molecular order control to be used in molecular electronic devices as either molecular platforms or as elements of circuitry.

3. EXPERIMENTAL SECTION

In this section of the Final Master Thesis the techniques, equipment and procedures utilised during the realization of this work will be presented and explained.

3.1 Compound studied.

A compound from the family of the curcuminoids (compound **1**, Figure 1) has been studied both at the air-water interface (Langmuir films) and once transferred onto a solid support (Langmuir-Blodgett (LB) or Langmuir-Schaefer (LS) films). Compound **1** was synthesized by Prof. Nuria Aliaga from the FunNanoSurf group at the ICMAB-CSIC in Barcelona in the framework of a collaboration with Prof. Pilar Cea at the Institute of Nanoscience and Materials Science of Aragón (INMA, CSIC-UNIZAR). Compound **1** incorporates the basic curcumin structure, formed by two aromatic rings connected by seven conjugated carbon atoms. Additionally, compound **1** also contains one boronic acid functional group at each aromatic ring, and a β-hydroxyketone in the connecting carbon chain.

Given the high conjugation shown by the molecule (Figure 1), compound **1** is expected to exhibit semiconducting properties due to the delocalized electrons in the π molecular orbital. Importantly, the terminal boronic acid groups allow for the formation of boroxine-like structures, giving rise to supramolecular ordering in the plane of the molecule.[17] Our hypothesis is that a monolayer of this molecule could exhibit in-plane electronic conductivity.

Compound **1** presents a brownish-orange colour, this molecule has a molecular mass of 363,96 g·mol^{-1}.

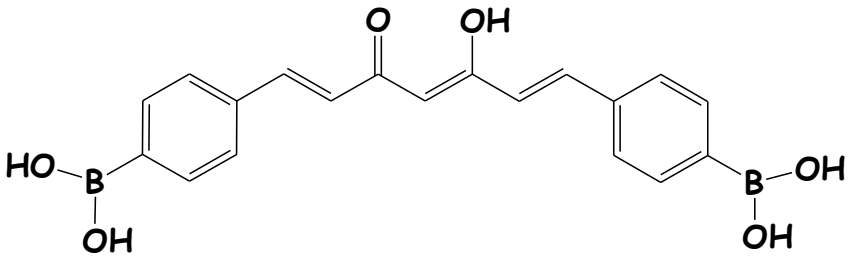

Figure 1. Molecular structure of compound **1**.

3.2 Substrates:

The substrates used in this work are shown in Table 1:

Table 1. Substrates used for the transference of monolayers of compound **1** formed at the air-water interface.

Substrate	Cleaning	Supplier
Mica	Mechanical exfoliation	Ted Pella Inc.
Gold-mica	As received	Georg Albert PVD Beschchtungen
Gold circuit on a silicon/silicon oxide substrate	As received	FunNanoSurf
Quartz Crystal Microbalance	Inmerse in $CHCl_3$ one hour and rinse with EtOH	QCM 25, Standford Research Systems
Quartz	$CHCl_3$ and EtOH ultrasound baths	Hellma Analytics

Mica is a highly hydrophilic substrate and very flat. This material is ideal for the deposition of monolayers for the subsequent exploration with Atomic Force Microscopy. Importantly, mica can be easily exfoliated using cello tape. Additionally, monolayers were also deposited on gold-on-mica substrates and on silicon/silicon oxide devices, Figure 2, which were prepared by the FunNanoSurf group. These substrates contain circuits having variable distances between the gold deposits.

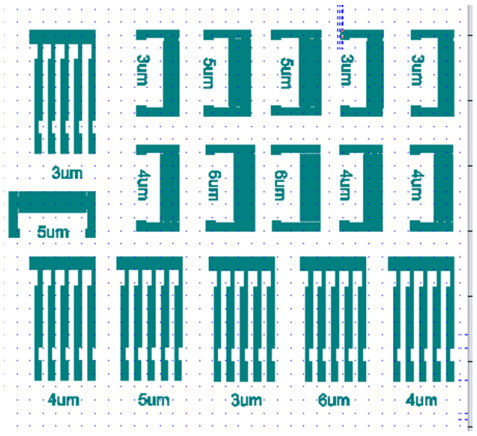

Figure 2. Patterned circuit used for carrying out the conductance measurements. The white background is made of silicon oxide and the blue areas are gold deposits.

3.3 Reactants:

Table 2. Reactants used.

Reactant	Molecular formula	Molecular weight ($g \cdot mol^{-1}$)	Function	Commercial information
Chloroform	$CHCl_3$	119.38	Solvent and cleaning agent	Macron, Fine Chemicals. Ethanol stabilized (1%)
Acetone	C_3H_6O	58.08	Cleaning agent	Fisher Chemical 99.8 %
Ethanol	C_2H_6O	46.07	Solvent	PanReac, AppliChem Absolute
Milli-Q water	H_2O	18.02	Cleaning agent and subphase	Millipore Milli-Q Plus

3.4 Equipment

Three different Langmuir troughs have been used for the realization of this work. Table 3 provides detailed information about these Langmuir troughs.

Table 3. Langmuir troughs used during this work.

Langmuir trough	*NIMA model 702*	*KSV-NIMA model KN 2003*	*KSV2000 system 3*
Dimensions	720 x 100 mm	580 x 145 mm	775 x 120 mm
Dipper for transferences	No	Yes	Yes
Other complementary *in-situ* techniques	Surface potential, BAM, UV-Visible Reflection spectroscopy	Vacuum attachment to perform Langmuir-Schaefer	-

The troughs are located inside a semi clean room and under stable environmental conditions, at 21 ± 1 °C with a relative humidity in the 50 to 60 % range.

To perform the surface potential measurements, a KSV-NIMA surface potential measurer was used that allows for the simultaneous registration of ΔV-A isothermand the π-A isotherm upon the compression process using the NIMA model 702.

Similarly, to obtain the Brewster Angle Microscopy (BAM) images, a KSV NIMA microBAM is mounted onto the NIMA model 702. The BAM employed makes use of a red laser of λ = 659 nm with a power of 50 mW and the reflected beam is recorded by a CCD camera of 640 x 480 pixels with a lateral resolution of 12 µm. In addition, the *in-situ* UV-Visible reflection spectra were registered with a NanofilmRefSpec2 reflection spectrophotometer equipped with a FiberLight DTM 6/50 lamp.

The instrument used to perform the UV-Visible spectroscopy measurements was a Varian Cary 50 Bio UV-VIS spectrophotometer. The cuvettes used were quartz cuvettes with a light path of 1 cm commercialized by Hellma Analytics, 100-QS.

To determine the topography of the transferred monolayers, an Atomic Force Microscope was used, the measurements were performed using a Multimode 5 or 8, from the Laboratory of Advanced Microscopies (LMA) equipped with a Nanoscope V control unit from Veeco.

3.5 Monolayer formation

3.5.1 Langmuir films:

The formation of a Langmuir film is achieved by spreading a solution of the molecule to be studied onto a water subphase, using a solvent (or mixture of solvents) immiscible with the liquid in the underlying subphase. The solvent should also have a positive and preferable large spreading coefficient onto the liquid in the subphase. With the help of a Hamilton syringe, the solution is carefully spread onto the water; the drops remain on top of the liquid phase due to the surface tension of water, even though they might have a higher density.

Before performing the experiments at the air-water interface though, it is necessary to properly clean the surface of the Langmuir trough. To achieve this, the trough is first rubbed with a paper towel with acetone and then, after all the acetone has been evaporated, the process is repeated but using chloroform instead. Both steps are aimed at retiring any possible residue from the trough. Additionally, the $CHCl_3$ also achieves a secondary goal: making the surface of the trough more hydrophobic.

As mentioned above, the preferred solvents for the preparation of the compound solution are those that have great spreading coefficients onto the subphase, which is typically water, and that also have a low boiling point, so they evaporate away as soon as possible. These are the reasons why chloroform is the most widely used solvent in the Langmuir technique, given its low boiling point, 63 °C, combined with a high spreading coefficient on water of 13.1 ergcm^{-2}. The studied curcuminoid, compound **1**, could not be dissolved completely into pure chloroform, so a mixture of chloroform and ethanol 4:1 was used instead, maintaining a high spreading coefficient, with a low boiling point while also being able to properly dissolve the molecule.

After the desired amount of volume has been spread, the solvent is allowed to be evaporated for 15 minutes, before the compression process starts. Upon this compression process the area available for the molecules is gradually reduced by means of superficial barriers that get closer to one another with a constant speed at 8 cm^2·min^{-1} (Figure 3).

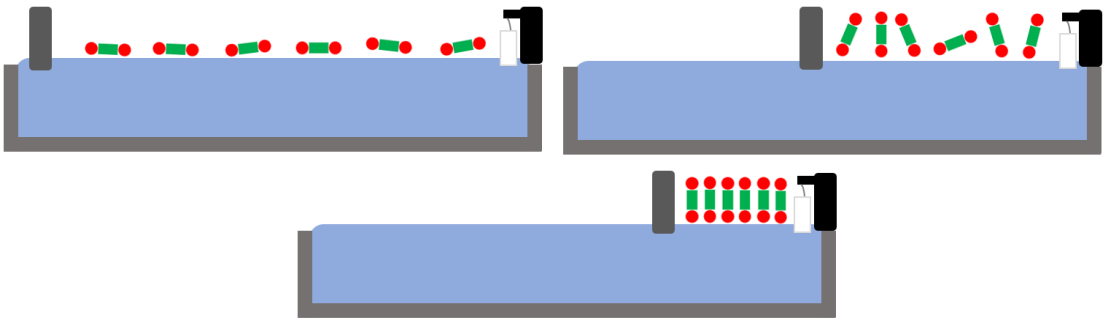

Figure 3. Compression process for the formation of a Langmuir monolayer at the air-water interface.

3.5.2 Langmuir-Blodgett films:

Once the Langmuir monolayer has been formed and has reached the target surface pressure or area per molecule value, it is possible to transfer it onto a solid substrate by performing what is known as a Langmuir-Blodgett (LB) transference. This procedure consists of either immersing (top to bottom) or emerging (bottom to top) the solid substrate through the Langmuir monolayer at a known and constant rate, thus transferring the monolayer onto the solid substrate, as seen in Figure 4. Depending on the direction in which the movement is performed, the molecules will be put in contact with the substrate by their water-loving functional groups or by their air-loving functional groups. In this work, all transferences have been made by the withdrawal of the substrate at a constant rate of 1 mm·min^{-1}.

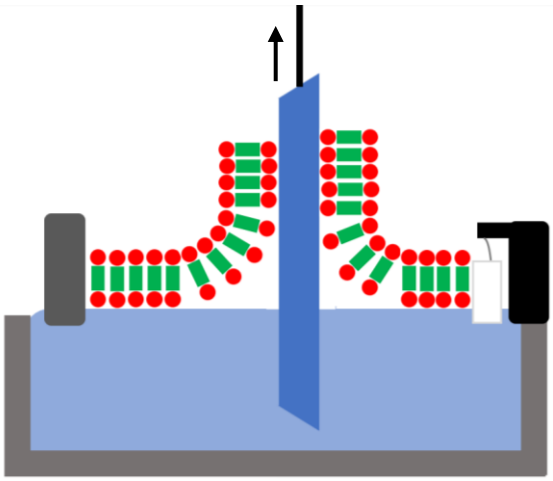

Figure 4. Illustration of the working procedure of a Langmuir-Blodgett transference.

LB is such a powerful technique because it allows for very fine control of the degree of order of the monolayer, while multi-layered systems with controlled thickness by repeating the transferring process can also be created. Since the monolayer deposition relies on physisorption (although chemisorption may also occur), a large number of substrate-anchoring group combinations can be used.

3.5.3 Langmuir-Schaefer:

Langmuir-Schaefer (LS) is based on the contact of the substrate with the water in a horizontal manner, so that the monolayer is deposited onto the substrate, as illustrated in Figure 5. The procedure consists in holding the back of the substrate by means of a vacuum generated by a mechanical pump. The LS transferences have been made by displacing the substrate at a rate of 1 $mm \cdot min^{-1}$.

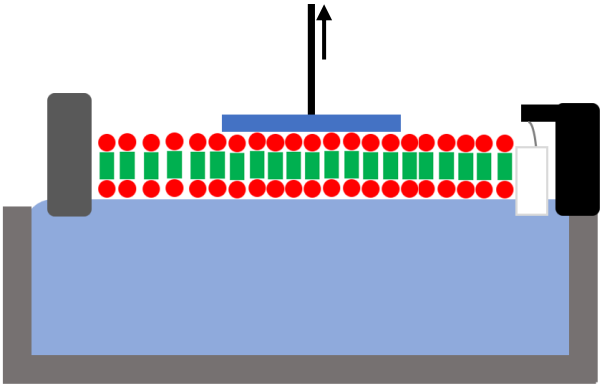

Figure 5. Illustration of the working procedure of a Langmuir-Schaefer transference.

3.6 Characterization techniques at the air-water interface

3.6.1 Surface pressure vs area per molecule isotherms

The surface pressure vs. the area per molecule of the Langmuir films can be recorded upon the compression process resulting in the so-called π-*A* isotherms. The surface pressure is defined as the difference between the surface tension of water (γ_0), and the surface tension at any given point in time (γ) upon the compression process.

$$\pi = \gamma_0 - \gamma \qquad \text{Equation 1}$$

In this work the surface pressure was determined by using a Wilhelmy microbalance, consisting of a thin plate (paper in our case) of known dimensions that is put in contact with the water subphase, until it is completely wetted.

These isotherms show the different aggregation states that the molecules go through during the compression. The surface pressure reached as well as the area per molecule recorded when the surface pressure started rising are characteristic properties of the molecule being studied, as well as the general shape of the curve: different slopes and presence or absence of plateaus.

The aggregation states that the molecules go through when forming the monolayer during compression include (although not all monolayers show all these phases and phase transitions) (Figure 6):

- Gas phase (G): molecules have so much area available that they hardly interact with each other and are free to have any possible orientation.
- Liquid Expanded (LE): even though molecules still have relatively large surface area available, they start interacting with the other molecules at the interface.
- Liquid Condensed (LC): given the lower area available per molecule, they start interacting heavily with each other. The monolayer is now starting to be formed.
- Solid phase (S): the monolayer is completely formed, and all molecules are fully oriented and arranged.
- Collapse (C): once the monolayer is fully formed, if the area is reduced further, it will collapse, starting the formation of multilayers.

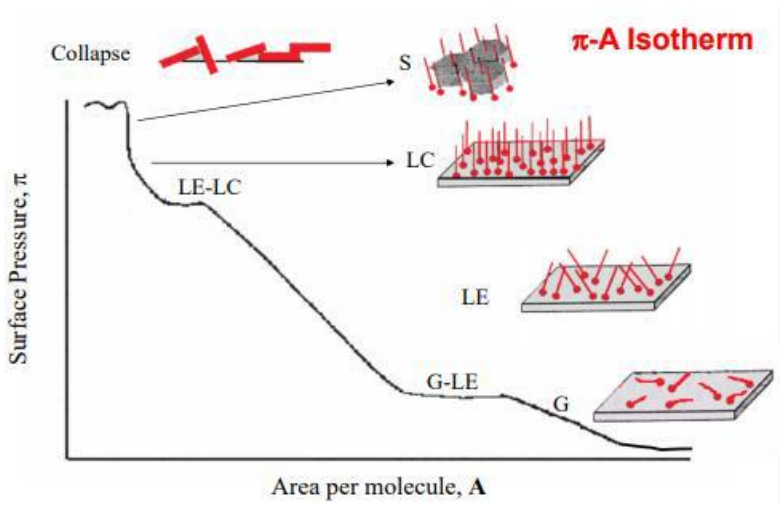

Figure 6. Phases and phase transitions of a typical Langmuir monolayer upon the compression process.

3.6.2 Surface potential vs. area per molecule isotherms

The changes of the surface potential of the monolayer upon the compression process can be recorded resulting in the surface potential vs. area per molecule isotherm, ΔV-A. This is possible by using a vibrating plate electrode put as close as possible to the liquid surface and another electrode placed inside the subphase, directly below the monolayer.

The vibrating electrode has a frequency of 140 Hz, and its movement is parallel to the plane of the liquid. The system works by keeping the capacitance constant, while variations in potential caused by the formation of the Langmuir monolayer are recorded thanks to the proportional changes in the measured current. This working principle can be seen in the scheme in Figure 7.

As shown in Equation 2, the changes in surface potential are related to the different apparent dipole moments of the molecule that appear as the barriers are compressed.

$$\Delta V = \frac{\mu}{A \cdot \varepsilon_0 \cdot \varepsilon} \qquad \text{Equation 2}$$

where A (m^2) is the area per molecule at any given moment, μ ($C \cdot m$) is the perpendicular component of the dipole moment of the molecules and ε_0 and ε ($C^2 \cdot N^{-1} \cdot m^2$) are the permittivity of both vacuum and the liquid.

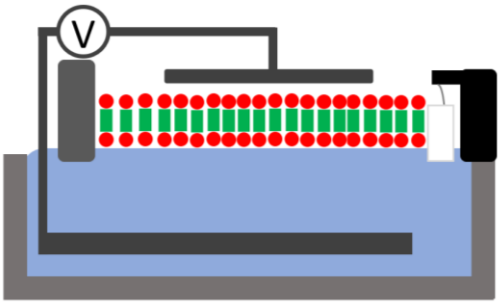

Figure 7. Schematics of the surface potential attachment for the NIMA trough.

3.6.3 Brewster angle microscopy (BAM):

This characterization technique allows for the direct observation of the formation of the Langmuir monolayers in real-time, while the monolayer is being formed. In this technique a beam of light polarized in the plane parallel to the incidence plane is shone into the subphase. At a specific angle, all the light that reaches the surface of the liquid is completely transmitted and no light is reflected into the air; this angle is known as the Brewster angle and the detector of the microscope does not detect any light (black image), Figure 8. This angle (53 °, for a pure water surface) is maintained constant in the microscope.

After spreading the molecules and once the barriers have started the compression process, the refraction index of the liquid changes, due to the formation of the monolayer, and light starts being reflected into the microscope in the areas where the monolayer has been already formed (Figure 8). Therefore, the BAM images provide visual information on the different phases of the Langmuir film, the formation of domains as well as the collapse of the monolayer.

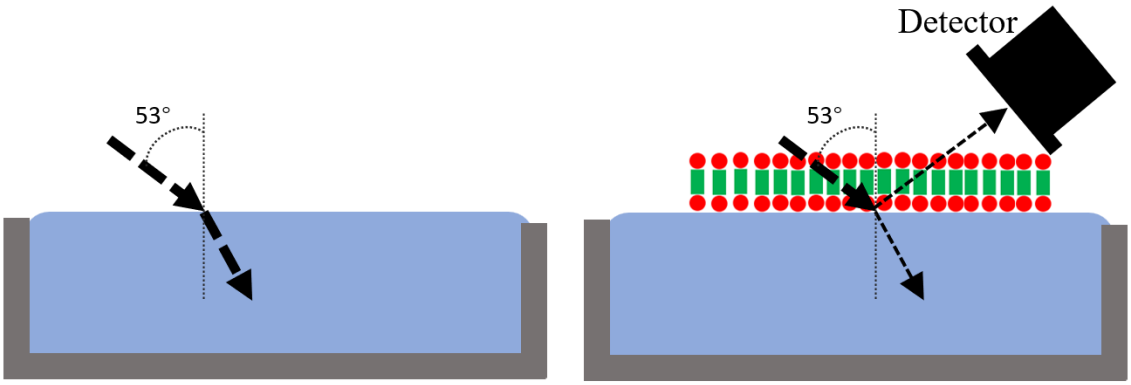

Figure 8. Illustration of the working principle of BAM.

3.6.4 UV-Visible Reflection Spectroscopy

In this technique, a non-polarized beam is incident on the surface of the water in the Langmuir trough in a perpendicular manner, with a fraction of the light being reflected and registered by a spectrophotometer. The reflected light depends on the presence or absence of the monolayer, as well as on its characteristics.

UV-Visible reflection spectroscopy provides *in-situ* information about the formation of the Langmuir film, the molecular orientation, or the formation of aggregates.

3.7 Characterization once transferred onto solid supports

3.7.1 Atomic Force Microscopy

Atomic Force Microscopy (AFM) is a sensitive technique that collects topographical information from the sample through the interaction of a very sharp tip whose radius of curvature is on the order of the nanometres, attached to a cantilever which, in turn, is connected to a set of piezoelectric devices. A laser is projected onto the back of the cantilever whose reflection is collected in a photodetector, translating the movements of the tip into voltages and making it possible to represent the surface of interest with very high resolution by performing successive sweeps that map the region of the sample under study (Figure 9). The main advantage of this force microscopy over other related microscopies such as Scanning Tunnelling Microscopy (STM) is that measurements can be performed on non-conductive samples, so all kinds of surfaces can be studied with none or minimal pre-treatment.

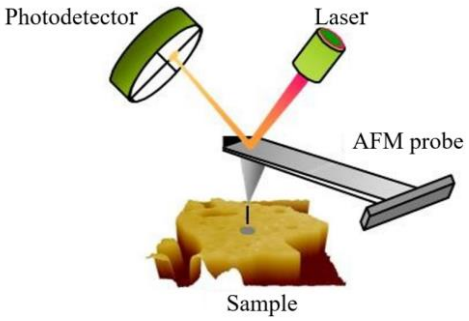

Figure 9. Schematics of the functioning of an AFM. [Adapted from[18]].

In this work the transferred monolayers have been studied by using intermittent contact mode, specifically *Tapping* mode.

In *Tapping* mode, the probe is oscillated at a frequency similar to its resonance frequency. Keeping a certain oscillation amplitude of the cantilever constant, a three-dimensional map of the surface of interest is obtained.

The AFM tips used in this work have been RTESPA-150, from *Bruker*, with a nominal resonance frequency of 150 kHz and a force constant of 6 $N \cdot m^{-1}$.

3.7.3 UV-Visible spectroscopy:

This technique allows to study the electronic states of molecules in solution or even when the material is transferred onto a solid. It works by irradiating the sample with a wide range of wavelengths and then registering the intensity of the light beam after it has interacted with the solution.

As mentioned above, this technique can be used to assess the absorptivity of the compound once it has been transferred onto a substrate forming a monolayer. To do this, the transference has to be performed onto a UV-Visible transparent substrate, in this case, quartz was used.

3.7.4 Quartz Crystal Microbalance

This technique makes use of the piezoelectricity properties exhibited by quartz when it is compressed or stretched. This phenomenon works in both ways, so that if an electric field is applied to quartz, it can change its dimensions. By applying an alternating electric field, it is possible to make a quartz substrate vibrate at its resonance frequency. This frequency is very sensitive to the mass of the substrate, so it changes after performing a deposition of molecules onto its surface. The equipment used was a Standford Research Systems model QCM200 microbalance with a QCM25 sensor. These substrates are circular quartz disks with gold electrodes on both sides and present a resonance frequency around 5 MHz.

4. EXPERIMENTAL RESULTS

4.1 Characterization of the compound in solution

The UV-Visible spectra of compound **1** in solution were recorded at several concentrations. The aim of these experiments was to find out in which concentration range the compound followed the Lambert-Beer Law, since a loss of linearity is indicative of the formation of 3D-aggregates. Compound **1** has a low solubility in chloroform, the most used solvent for Langmuir experiments. For this reason, it was dissolved in a mixture of chloroform:ethanol in a 4:1 ratio. After sonication for one minute, to further ensure the absence of aggregates, the solution was clear and exhibited a yellowish colour.

Figure 10(a) shows the UV-Visible spectra for compound **1** in the 10^{-4} M - $2.5 \cdot 10^{-6}$ M range. The UV-Visible spectrum of compound **1** features a wide band with a maximum at 398 nm. Figure 10(b) shows the absorbance at 398 nm vs. concentration, that exhibits a linear behaviour for the whole range of concentrations considered. This indicates that compound **1** does not form 3D-aggregates in this range of concentrations.

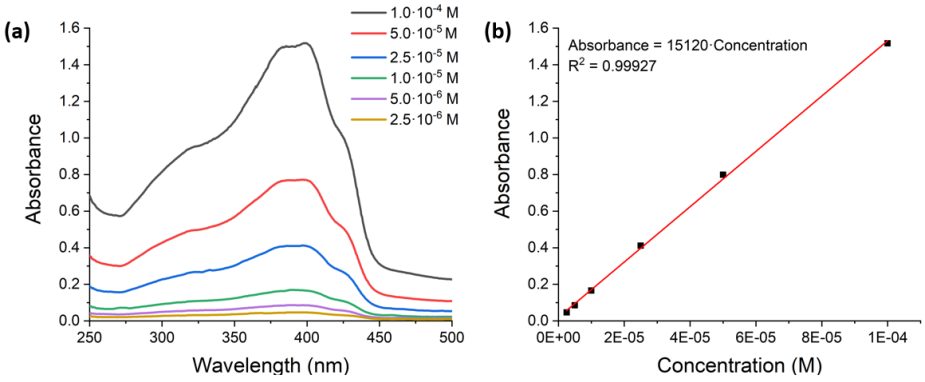

Figure 10. (a) UV-Visible spectra for compound **1** at the indicated concentrations. (b) Absorbance at 398 vs concentration of compound **1**.

According to the Lambert-Beer Law (Equation 3):

$$A = \varepsilon \cdot c \cdot l \qquad \text{Equation 3}$$

where A is the absorbance, ε is the molar absorptivity ($mol^{-1} \cdot L \cdot cm^{-1}$), c is the concentration (M), and l is the length of the optical pass of the cuvette (cm). The molar absorptivity of compound **1** is 15120 $mol^{-1} \cdot L \cdot cm^{-1}$ in the chloroform:ethanol 4:1 mixture, whilst this value is 17047 $mol^{-1} \cdot L \cdot cm^{-1}$ in ethanol; albeit this molar absorptivity value might seem low when compared to most curcuminoids,[19] there have been reports of other curcumin derivatives with similarly low molar absorptivities.[20,21] The inclusion of an

electron withdrawing group such as boronic acid, has been showed to have a lowering effect on the molar absorptivity for other conjugated molecules, the same effect might be happening with compound **1**.[22]

4.2 Fabrication and characterization of Langmuir films

A comprehensive study of compound **1** was performed to determine the optimal experimental conditions (concentration of the solution and spreading volume) to obtain reproducible isotherms for the formation of a monolayer at the air-water interface. From these experiments, it was concluded that a solution concentration of 10^{-5} M and a spreading volume of 8 mL yields reproducible isotherms (Figure 11(a)). The barriers were compressed at 8 $cm^2 \cdot min^{-1}$.

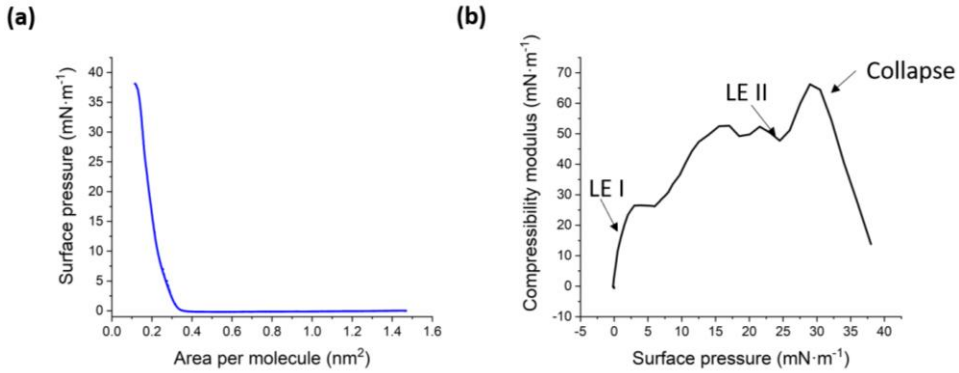

Figure 11. (a) Surface pressure vs area per molecule isotherm for compound **1**. (b) Compressibility modulus vs surface pressure.

In Figure 11(b), the compressibility modulus has been shown, calculated according to Equation 4:

$$K_s = -A \cdot \left(\frac{d\pi}{dA}\right)_{p,T} \qquad \text{Equation 4}$$

From Figure 11, it is possible to conclude that the isotherm can be divided into three regions. While the surface pressure remains at 0 $mN \cdot m^{-1}$, the Langmuir film shows a gas phase behaviour. Once the surface pressure starts increasing, it enters the Liquid-Expanded phase at approximately 5 $mN \cdot m^{-1}$, which according to the Davies and Rideal classification, exists for values of the compressibility modulus up to 50 $mN \cdot m^{-1}$. While in this phase, it undergoes phase changes still behaving as a Liquid-Expanded, as seen at 25 $mN \cdot m^{-1}$. Lastly, at 30 $mN \cdot m^{-1}$, the monolayer is at its most condensed state but upon

further reduction of the area per molecule, local and then general collapse of the film occurs.[23,24]

In addition to the π-*A* isotherm, the surface potential vs area per molecule (Δ*V*-*A*) isotherm was also recorded. This measurement is highly sensitive and can detect changes in the Langmuir film even before they appear in the π-*A* graph.

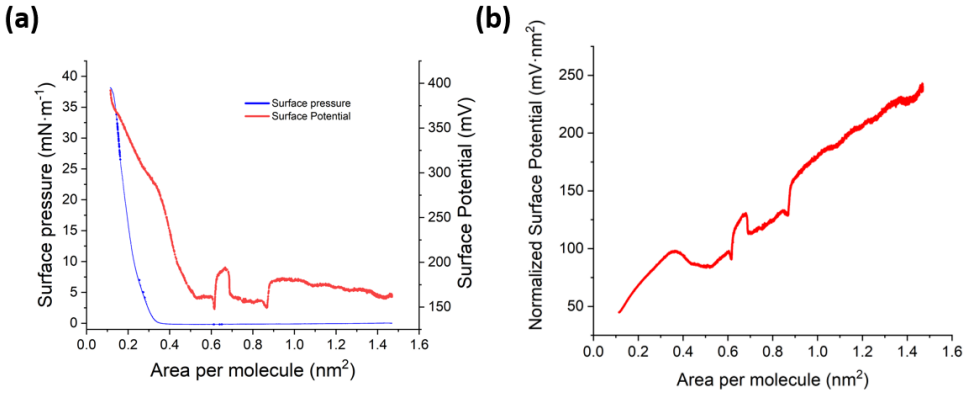

Figure 12. (a) Surface pressure and surface potential versus area per molecule isotherm. (b) Normalized surface potential versus area per molecule.

Figure 12(a) shows the surface potential isotherm for the Langmuir monolayer of compound **1** and Figure 12(b) shows the normalized surface potential for non-ionized films, defined as:[25]

$$\Delta V_n = \Delta V \cdot A \qquad \text{Equation 5}$$

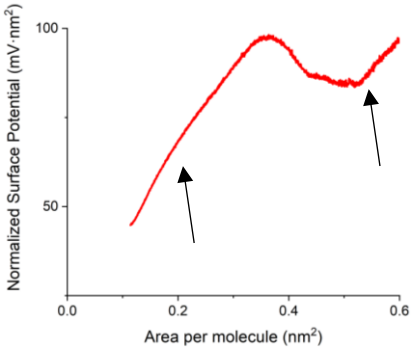

Figure 13. Detail from 0.0 to 0.6 nm^2 region of the normalized surface potential.

In non-ionized monolayers, as is the case here, the surface potential is directly proportional to the normal component of the dipole moment of the molecules, as shown in Equation 6:

$$\Delta V = \frac{\mu_n}{A \cdot \varepsilon_r \cdot \varepsilon_0} \qquad \text{Equation 6}$$

where ΔV is the surface potential; μ_n is the normal component of the dipole moment; A is the area per molecule and ε_r and ε_0 are the permittivities of water and vacuum, respectively.

In Figures 12(b) and 13, the real effect the compression process has on the surface potential is observed. There is a steady decrease in normalized surface potential upon compression, with certain artifacts such as minima and maxima that correspond to local changes in the Langmuir film in the gas phase, possibly due to the presence of domains distributed in a non-homogeneous manner on the water surface. At 0.55 nm^2 there is a change in slope that corresponds to the increase in surface pressure observed in the π-A isotherm, indicative of a Gas-Liquid Expanded I transition. The change in the sign of the slope observed at 0.35 nm^2 can be explained by another phase transition to a secondary Liquid Expanded phase (LE II), as seen in the compressibility modulus graph. At 0.2 nm^2 there is a subtle change in the slope, corresponding to the start of the collapse of the monolayer, first locally and then throughout the whole system.

To observe *in-situ* the formation of the Langmuir film upon the compression process, the Brewster Angle Microscopy (BAM) was used. Figure 14 shows the BAM images at the indicated surface pressures.

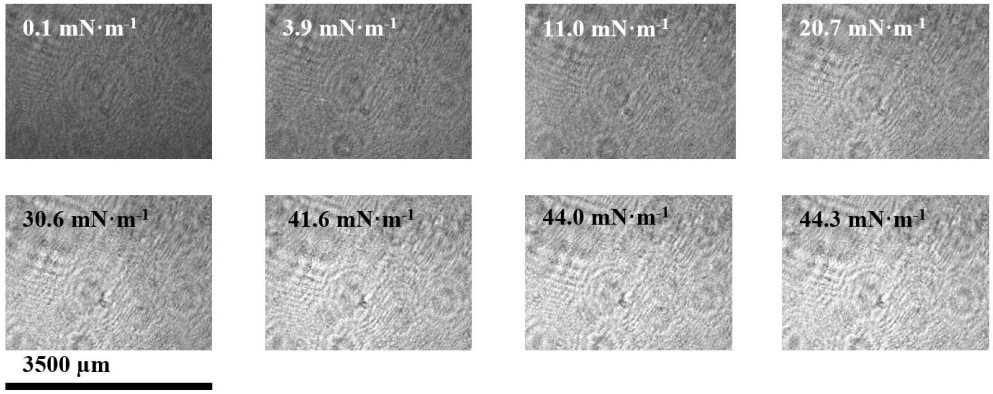

Figure 14. BAM images recorded upon the compression of the barriers at the indicated areas per molecule.

BAM images show the formation of a very homogeneous film upon compression; being the most remarkable observation the evolution of the images from dark grey to light grey, which is indicative of a larger surface density of compound **1** and/or even an increase in the thickness of the film.

Another useful technique that provides *in-situ* information about the behaviour of compound **1** at the air-water interface is UV-Visible reflection spectroscopy. For that,

several UV-Visible spectra are recorded upon the compression process, and they can be analysed to determine the formation of 2D-aggregates, or even to study the tilt angle of the molecules with respect to the water surface. Figure 15 shows the raw UV-Visible spectra at the indicated areas per molecule together with the absorbance spectrum registered at $1 \cdot 10^{-5}$ M, for comparison purposes.

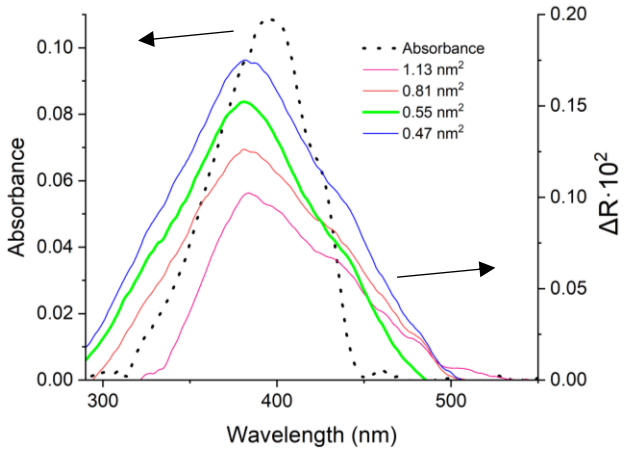

Figure 15. UV-Visible spectra registered upon the compression process at different areas per molecule and of **1** in a 10^{-5} M solution in $CHCl_3$:EtOH 4:1.

The broadening of the band when performing the measurement at the air-water interface points to the formation of 2D-aggregates containing different number of molecules. Moreover, the maximum of the peak is shifted from 392 nm in solution (chloroform:ethanol 4:1) to 383 nm at the air-water interface. This peak corresponds to the π-π* electronic transition of the conjugated system.[26] The hypsochromic shift at the air-water interface with respect to the solution could be interpreted in terms of (i) a change in the environment polarity or (ii) the formation of H-aggregates. Figure 16 shows the absorbance spectrum of the molecule in ethanol, with a maximum at 395 nm, which does not change after the addition of water (increasing the polarity of the medium). These results rule out hypothesis (i), with the observed hypsochromic shift of the maximum absorbance of compound **1** at the air-water interface being attributable to the formation of 2D H-aggregates.

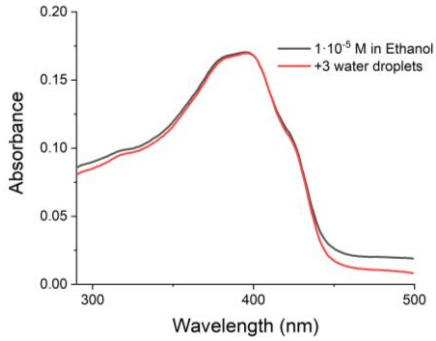

Figure 16. Black: absorbance spectrum of a $1 \cdot 10^{-5}$ M solution of compound **1** in ethanol. Red: spectrum of the same solution after adding 3 drops of water.

To add some light into the orientation changes of the molecule upon the compression process at the air-water interface, the UV-Visible reflection spectra were normalized to account for the surface density increase upon the compression process. To do so, the reflection values were multiplied by the area per molecule at which each spectrum was recorded ($\Delta R_n = \Delta R \cdot$ Area per molecule), as illustrated in Figure 17.

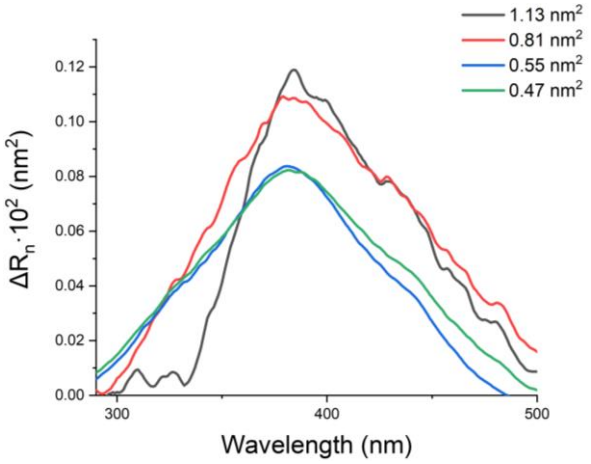

Figure 17. Normalized UV-Visible reflection spectra at the indicated areas per molecule upon the compression process.

The gradual decrease in the normalized reflection data from the initial area per molecule to a value of 0.55 nm^2 is indicative of a change in the orientation of the molecule upon the compression process, consisting of the gradual decrease of the angle between transition dipole moment of the molecule and the normal to the surface of water. Further compression of the monolayer does not result in a significant change in the reflection values, revealing no changes in the molecular orientation.

4.3 Fabrication and characterization of transferred films onto solid supports

After studying compound **1** at the air-water interface by means of π-*A* isotherms, Δ*V*-*A* isotherms, UV-Visible reflection spectroscopy and BAM, the films were transferred onto solid supports by using the Langmuir-Blodgett technique. This transference has been quantified using a Quartz Crystal Microbalance. The films were transferred onto QCM substrates and the change in the resonance frequency before and after the transference, provided quantitative information of the amount of material deposited. To get an idea of the ratio of transference of compound **1**, a monolayer was transferred at a target surface pressure of 10 $mN \cdot m^{-1}$, resulting in a frequency change of 16 Hz. This change in frequency can be related with the deposited mass by using the Sauerbrey equation (Equation 7).[27]

$$\Delta f = - C_f \cdot \Delta m \qquad \text{Equation 7}$$

where Δf is the change in frequency of oscillation of the quartz crystal, C_f is the sensitivity factor, with a value of 56.6 $Hz \cdot cm^2 \cdot \mu g^{-1}$, and Δm is the mass of material that has been deposited per surface area. The final mass change is 0.1413 $\mu g \cdot cm^{-2}$, which corresponds to a surface coverage of $3.88 \cdot 10^{-10}$ $mol \cdot cm^{-2}$. This value is significantly lower than the one obtained from the π-*A* isotherm at 10 $mN \cdot m^{-1}$, $7.26 \cdot 10^{-10}$ $mol \cdot cm^{-2}$. This could be due to either a poor ratio of transference of the molecule onto the QCM substrate or a change in the orientation of the molecules onto the solid support in comparison to the air-water interface or due to the formation of aggregates. In order to verify or rule out orientation effects, the UV-Visible spectrum of a LB monolayer of compound **1** at 10 $mN \cdot m^{-1}$ was determined and it is shown in Figure 18. The apparent molar absorptivities were plotted at each wavelength, calculated according to Equations 8 and 9.

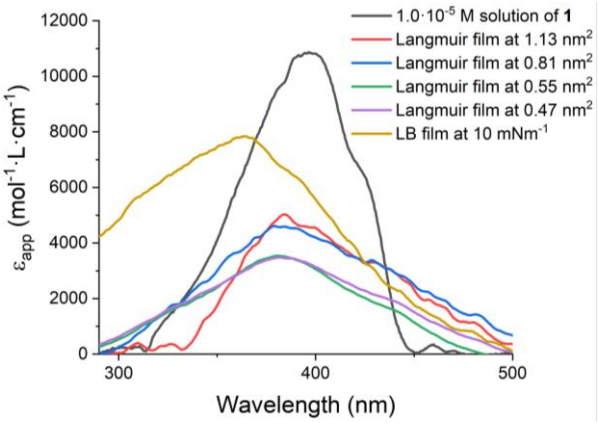

Figure 18. Molar absorptivity for a $1.0 \cdot 10^{-5}$ M solution of compound **1** and apparent molar absorptivities of compound **1** deposited onto a quartz substrate at 10 $mN \cdot m^{-1}$ and at the indicated areas per molecule upon the compression process.

$$\varepsilon_{app} = \frac{Abs}{1000 \cdot \Gamma} \qquad \text{Equation 8}$$

$$\varepsilon_{app} = \frac{\Delta R}{2{,}303 \cdot 10^3 \cdot \Gamma \cdot R_w^{\frac{1}{2}}} \qquad \text{Equation 9}$$

The decrease of intensity for the Langmuir and LB films, compared to the intensity showed by compound **1** in solution, is due to changes in orientation of the molecules upon the compression process and when transferring them onto the solid substrate.

The main peak of the compound is blue-shifted in the LB films compared to the Langmuir film and the solution. This is typical for the formation of H-aggregates, in which the molecules appear in a "plane-to-plane" configuration, confirming hypothesis (ii). In contrast, J-aggregates, in which the molecules are ordered in a "head-to-tail" manner, feature a bathochromic shift.[28]

To study the topography and morphology of the transferred films, atomic force microscopy was used onto deposits of compound **1** transferred at surface pressures that correspond to both Liquid Expanded phases, at 10 mN·m^{-1} and 30 mN·m^{-1}. Figure 19 shows the 2D images of LB films transferred at a surface pressure of 10 mN·m^{-1} onto freshly cleaved mica substrates.

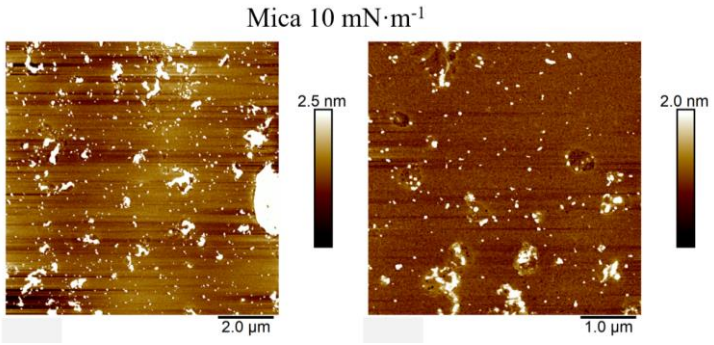

Figure 19. AFM images of monolayers of compound **1** transferred onto mica substrates at a surface pressure of 10 mN·m^{-1}.

These deposits show an underlying monolayer of molecules, on top of which aggregates with irregular shapes and distribution can be observed. These aggregates are attributed to local collapses of the monolayer during the transference process. A similar situation can be observed for the transferences made at 30 mN·m^{-1} (Figure 20), with an even higher concentration of aggregates.

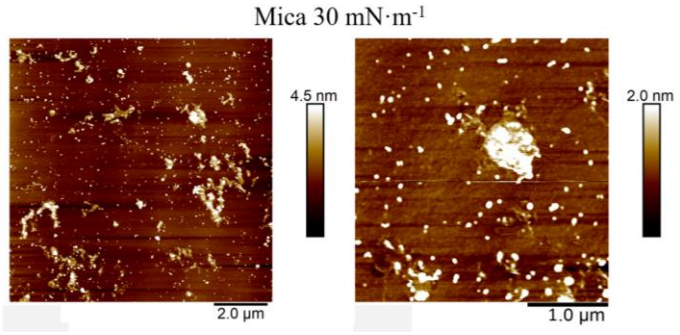

Figure 20. AFM images of one LB layer transferred onto a mica substrate at a surface pressure of 30 $mN \cdot m^{-1}$.

As indicated previously, the ultimate objective of this work is to test the electrical response of a deposited layer of compound **1**. For that, LB films will be deposited over silicon/silicon oxide with printed gold electrical contacts substrates provided by the research group FunNanoSurf (Prof. Nuria Aliaga at ICMAB, Barcelona). For this reason, the morphology of the LB layers transferred onto gold was also analysed. The transferences were made at 10 $mN \cdot m^{-1}$ and 30 $mN \cdot m^{-1}$ onto gold-on-mica substrates (Figure 21).

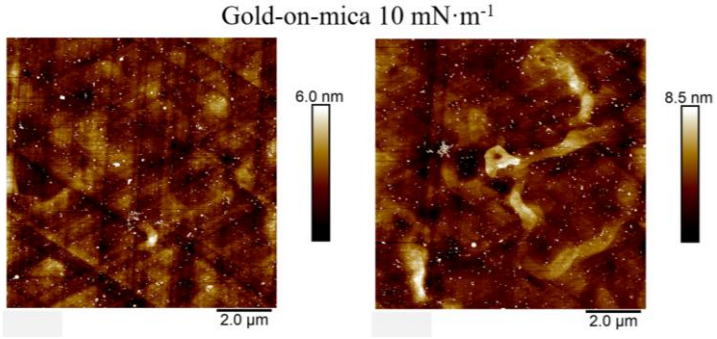

Figure 21. AFM images of a LB layer of compound **1** deposited onto gold-on-mica substrates at 10 $mN \cdot m^{-1}$.

Importantly, the homogeneity of the deposit is much higher on gold-on-mica substrates when compared to the mica substrates, which is attributable to a different interaction of compound **1** with both substrates. The underlying structure of gold, with terraces of Au(111) can be seen in these images (Figure 21), but they are clearly coated with a thin layer of molecules. Certain aggregates can be seen throughout the image, but most of the area is covered by the mentioned deposit of molecules. The LB layer transferred at 30 $mN \cdot m^{-1}$ is also relatively homogeneous although with the presence of some aggregates on the surface (Figure 22).

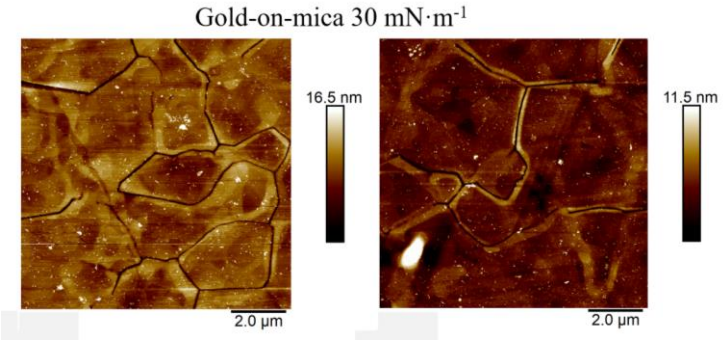

Figure 22. AFM images of a LB layer of compound **1** deposited onto gold-on-mica substrates at 30 $mN \cdot m^{-1}$.

Following these results, the transferences were then carried out onto the silicon/silicon oxide printed devices at 10 $mN \cdot m^{-1}$ by LB, Figure 23.

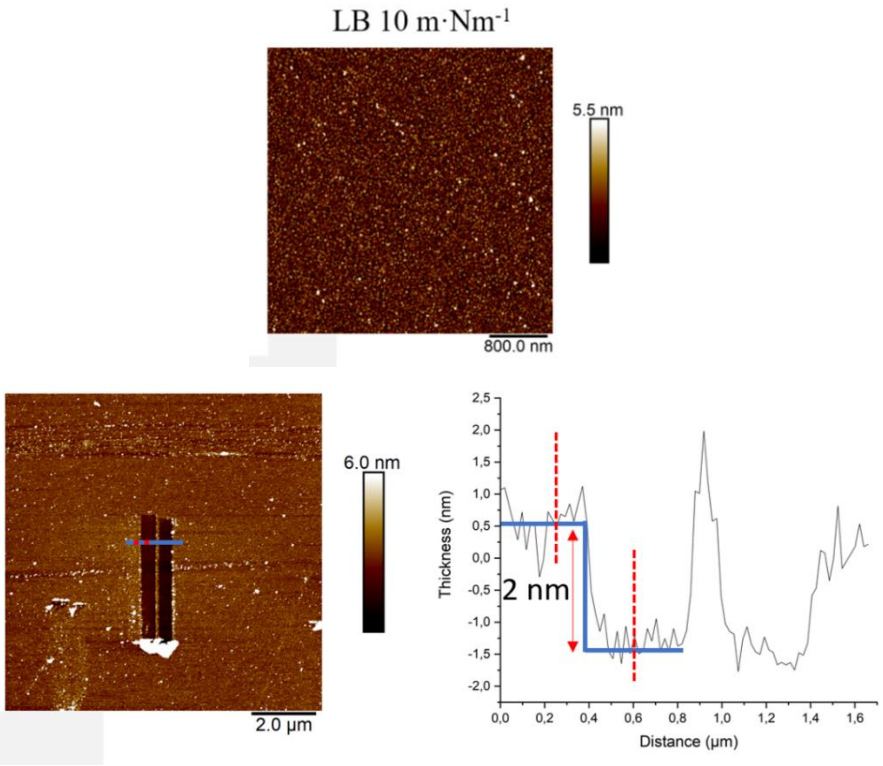

Figure 23. Top: AFM image of a LB layer of compound **1** transferred onto silicon/silicon oxide at 10 $mN \cdot m^{-1}$. Bottom: image of a scratched area (AFM nanolithography) of the film and its profile.

According to the literature, in some cases LS is preferred over LB because it might lead to the formation of fewer aggregates.[29] To make sure that the transferences were being done by the technique that yielded the most homogeneous deposits, transferences

were also performed by LS onto the silicon/silicon oxide substrates at 10 $mN \cdot m^{-1}$, Figure 24.

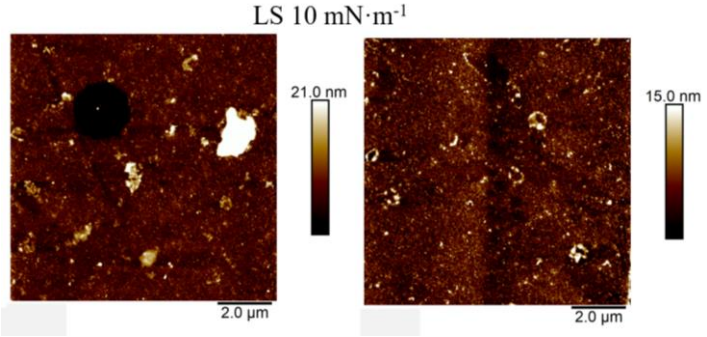

Figure 24. AFM image of a LS monolayer of compound **1** onto silicon/silicon oxide transferred at 10 $mN \cdot m^{-1}$.

These experiments demonstrated that while the deposits made by LB are homogeneous and show a rather limited number of 3D-aggregates when made onto the silicon/silicon oxide substrates (Figure 23), those obtained by LS contain more aggregates of bigger size (Figure 24). For this reason, henceforward we used the LB technique for the transference of compound **1**.

For comparison purposes, Figure 25, shows the AFM images of a LB monolayer of compound **1** transferred onto different substrates at 10 $mN \cdot m^{-1}$. It is important to remark that in this particular case, the nature of the substrate has a large influence on the morphology of the resulting LB layer.

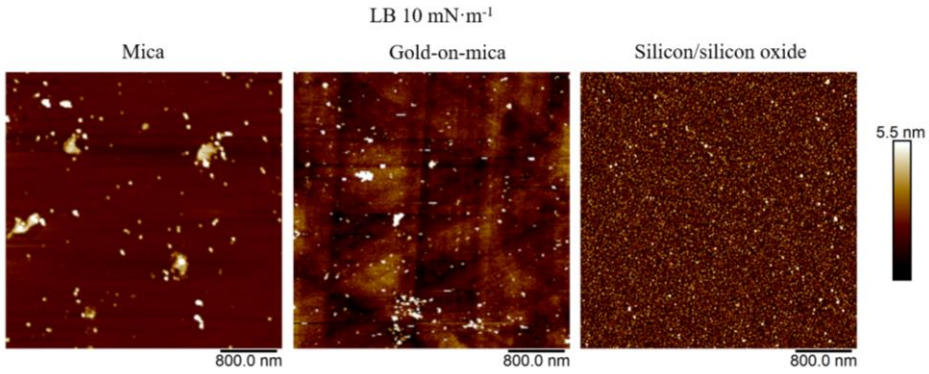

Figure 25. AFM images of a LB monolayer of compound **1** transferred onto the indicated substrates at a target surface pressure of 10 $mN \cdot m^{-1}$.

After studying the previous images, the conclusion reached was that the molecules were orienting themselves perpendicular to the surface of the substrate, given the height of the profile of the scratched image (Figure 23) and the small areas per molecule at which

the transferences were made (around 0.2 nm^2). In hopes of obtaining the molecules arranged in a planar manner towards the substrate (Figure 26), more transferences were made at a higher area per molecule, specifically at 2.6 nm^2. These transferences were done onto gold-on-mica substrates by LB and the resulting deposits were modified by AFM lithography to determine the height of the layer of compound **1**.

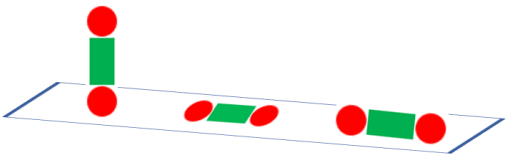

Figure 26. Left: perpendicular orientation of the molecules. Centre: planar orientation of the molecules. Right: orthogonal orientation of the molecules

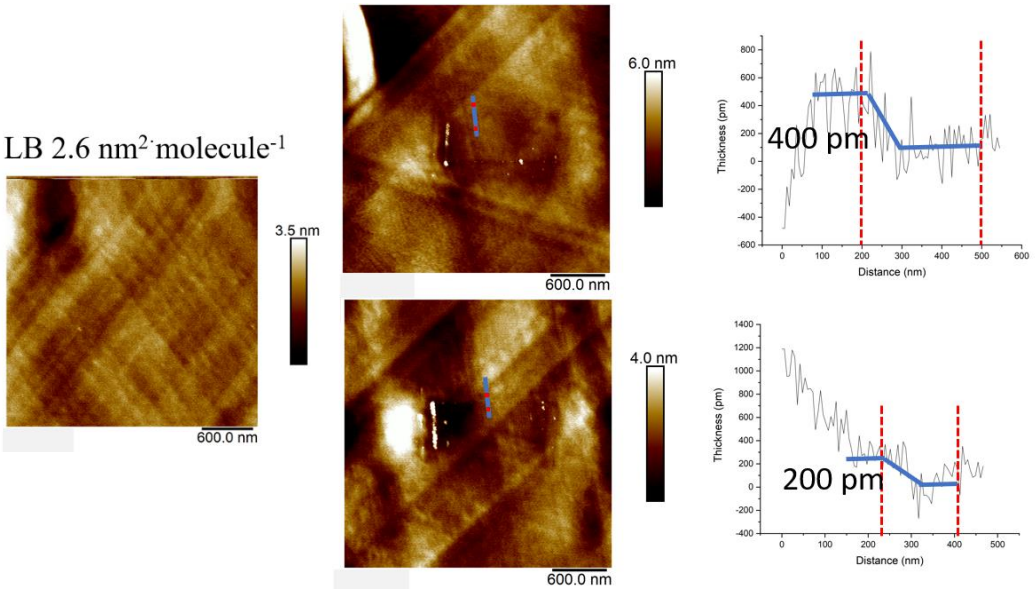

Figure 27. Left: AFM image of the gold-on-mica substrate once the monolayer of compound **1** was transferred at 2.6 $nm^2 \cdot molecule^{-1}$ by LB. Middle and right: images of scratched areas of the same characteristics, prepared by AFM lithography, and their profiles.

As can be seen in the images shown in Figure 27, the deposit is very homogeneous, and no aggregates are formed. The differences in height between the scratched area and the surrounding surfaces are in the range of the diameter of a carbon atom (170 pm), revealing a flat orientation of the molecules in these films.

Once the LB films were deposited onto the silicon/silicon oxide with printed gold electrical contacts substrates, conductance measurements were carried out by Rossella

Zaffino at Dr. Aliaga's research group. The aim of these experiments was to shed light on the electronic behaviour of compound **1** depending on the molecular orientation.

Several conductance measurements were performed using a Keithley 2450 and a homemade python script to obtain current values both at ambient pressure and under vacuum, at each of the different gold contacts (see Figure 2). The highest conductance was obtained for the most homogeneous deposit, transferred at 10 $mN \cdot m^{-1}$ by Langmuir-Blodgett (Figure 28). Nevertheless, even when the obtained results are promising, more work needs to be done to understand much better the conductance behaviour of compound **1**.

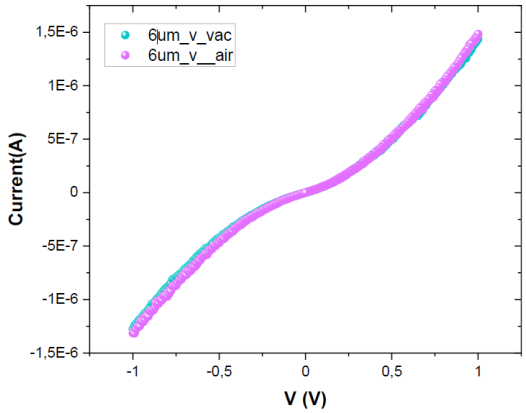

Figure 28. I-V curves registered at ambient pressure and vacuum for compound **1** deposited on the silicon/silicon oxide devices at 10 $mN \cdot m^{-1}$ by LB. The distance between the gold electrodes is 6 µm.

5. CONCLUSIONS AND FUTURE PERSPECTIVES

Langmuir films of compound **1** at the air-water interface have been obtained and comprehensively characterized by means of π-*A* and Δ*V*-*A* isotherms, Brewster Angle Microscopy and UV-Visible reflection spectroscopy. Compound **1** shows a reproducible surface activity and forms homogeneous fluid monolayers (liquid expanded state even at high surface pressures) exhibiting a gradual tilt of the transition dipole moment upon compression during the gas phase, and formation of H-aggregates incorporating different number of n-meres. These monolayers have been transferred onto solid supports, although a decrease in the surface density upon the transference process occurs. A further blue-shift of the π-π* transition band in the UV-Visible spectrum is observed after the transference, indicative of a further reorganization of the molecules. AFM images confirm the presence of a layer of approximately 2 nm in thickness when the compound was transferred at 10 $mN \cdot m^{-1}$, revealing a molecular orientation perpendicular to the surface of the substrate. Moreover, when transferring at higher surface pressure values (lower areas per molecule) the films are not as homogeneous and the formation of aggregates is enhanced. On the contrary, when the transferences are made at higher areas per molecule, 2.6 nm^2, very homogenous films, practically without the presence of aggregates and with a thickness smaller than 0.5 nm are obtained. This latter result indicates that the molecules of compound **1** are located in a planar manner with respect to the surface of the substrate.

Once the control of the orientation of the molecules seems to be achieved and preliminary conductance measurements on silicon/silicon oxide with printed gold electrical contacts substrates obtained, a future perspective for this research line is to test the electrical properties as a function of the molecular orientation. Future studies also include the formation of 2D COFs of compound **1**, perhaps by changing the terminal groups in the same curcuminoid moiety.

6. BIBLIOGRAPHY

(1) Gordon E. Moore. Cramming More Components onto Integrated Circuits. *Electronics (Basel)* **1965**, *38* (8), 114–117.

(2) Gordon E. Moore. Progress in Digital Integrated Electronics; International Electron Devices Meeting, IEDM Technical Digest, **1975**; 11–13.

(3) Wallace Witkowski. *'Moore's Law's dead,' Nvidia CEO Jensen Huang says in justifying gaming-card price hike*. MarketWatch.

(4) Maruccio, G.; Cingolani, R.; Rinaldi, R. Projecting the Nanoworld: Concepts, Results and Perspectives of Molecular Electronics. *J. Mater. Chem.* **2004**, *4*, 542–554. https://doi.org/10.1039/b311929g.

(5) Martín-Barreiro, A.; Soto, R.; Chiodini, S.; García-Serrano, A.; Martín, S.; Herrer, L.; Pérez-Murano, F.; Low, P. J.; Serrano, J. L.; de Marcos, S.; Galban, J.; Cea, P. Uncapped Gold Nanoparticles for the Metallization of Organic Monolayers. *Adv. Mater. Interfaces* **2021**, *8* (18), 2100876. https://doi.org/10.1002/admi.202100876.

(6) Hsu, L. Y.; Jin, B. Y.; Chen, C. hsien; Peng, S. M. Reaction: New Insights into Molecular Electronics. *Chem*. **2017**, 3 (3), 378–379. https://doi.org/10.1016/j.chempr.2017.08.007.

(7) Sun, L.; Diaz-Fernandez, Y. A.; Gschneidtner, T. A.; Westerlund, F.; Lara-Avila, S.; Moth-Poulsen, K. Single-Molecule Electronics: From Chemical Design to Functional Devices. *Chem. Soc. Rev.* **2014**, *21,* 7378–7411. https://doi.org/10.1039/c4cs00143e.

(8) Novikov, V. N.; Sokolov, A. P. Poisson's Ratio and the Fragility of Glass-Forming Liquids. *Nature* **2004**, *431* (7011), 961–963. https://doi.org/10.1038/nature02947.

(9) Gao, M.; Shih, C. C.; Pan, S. Y.; Chueh, C. C.; Chen, W. C. Advances and Challenges of Green Materials for Electronics and Energy Storage Applications: From Design to End-of-Life Recovery. *J. Mater. Chem. A*. **2018**, *42,* 20546–20563. https://doi.org/10.1039/C8TA07246A.

(10) Wang, S.; Oh, J. Y.; Xu, J.; Tran, H.; Bao, Z. Skin-Inspired Electronics: An Emerging Paradigm. *Acc. Chem. Res.* **2018**, *51* (5), 1033–1045. https://doi.org/10.1021/acs.accounts.8b00015.

(11) Xin, N.; Guan, J.; Zhou, C.; Chen, X.; Gu, C.; Li, Y.; Ratner, M. A.; Nitzan, A.; Stoddart, J. F.; Guo, X. Concepts in the Design and Engineering of Single-

Molecule Electronic Devices. *Nat. Rev. Phys*. **2019**, *1,* 211–230. https://doi.org/10.1038/s42254-019-0022-x.

(12) Escorihuela, E.; Cea, P.; Bock, S.; Milan, D. C.; Naghibi, S.; Osorio, H. M.; Nichols, R. J.; Low, P. J.; Martin, S. Towards the Design of Effective Multipodal Contacts for Use in the Construction of Langmuir-Blodgett Films and Molecular Junctions. *J. Mater. Chem. C Mater.* **2020**, *8* (2), 672–682. https://doi.org/10.1039/c9tc04710g.

(13) Cea, P.; Ballesteros, L. M.; Martín, S. Nanofabrication Techniques of Highly Organized Monolayers Sandwiched between Two Electrodes for Molecular Electronics. *Nanofabrication* **2014**, *1* (1), 96-117. https://doi.org/10.2478/nanofab-2014-0010.

(14) Guan, X.; Chen, F.; Fang, Q.; Qiu, S. Design and Applications of Three Dimensional Covalent Organic Frameworks. *Chem. Soc. Rev.* **2020**, *5,* 1357–1384. https://doi.org/10.1039/c9cs00911f.

(15) Meng, Z.; Stolz, R. M.; Mirica, K. A. Two-Dimensional Chemiresistive Covalent Organic Framework with High Intrinsic Conductivity. *J. Am. Chem. Soc.* **2019**, *141* (30), 11929–11937. https://doi.org/10.1021/jacs.9b03441.

(16) Escorihuela, E.; Concellón, A.; Marín, I.; Kumar, V. J.; Herrer, L.; Moggach, S. A.; Vezzoli, A.; Nichols, R. J.; Low, P. J.; Cea, P.; Serrano, J. L.; Martín, S. Building Large-Scale Unimolecular Scaffolding for Electronic Devices. *Mater. Today Chem.* **2022**, *26,* 101067. https://doi.org/10.1016/j.mtchem.2022.101067.

(17) Li, H.; Li, H.; Dai, Q.; Li, H.; Brédas, J. L. Hydrolytic Stability of Boronate Ester-Linked Covalent Organic Frameworks. *Adv Theory Simul* **2018**, *1* (2), 1700015. https://doi.org/10.1002/adts.201700015.

(18) González Orive, A. Tesis Doctoral, Electrogeneración de Películas Ultradelgadas de Melanina : Nanoestructura, Electrocatálisis, Conductividad, Magnetismo y Fotorrespuesta. *Servicio de Publicaciones, Universidad de La Laguna*.

(19) Dotor, L.; García-Pinilla, J. M.; Martín, S.; Cea, P. Langmuir and Langmuir-Blodgett Technologies as Nanoarchitectonic Tools for the Incorporation of Curcumin in Membrane Systems. *Nanoscale* **2023**, *15* (6), 2891–2903. https://doi.org/10.1039/d2nr06631a.

(20) Rodrigues, F. M. S.; Tavares, I.; Aroso, R. T.; Dias, L. D.; Domingos, C. V.; de Faria, C. M. G.; Piccirillo, G.; Maria, T. M. R.; Carrilho, R. M. B.; Bagnato, V. S.; Calvete, M. J. F.; Pereira, M. M. Photoantibacterial Poly(Vinyl)Chloride Films

Applying Curcumin Derivatives as Bio-Based Plasticizers and Photosensitizers. *Molecules* **2023**, *28* (5), 2209. https://doi.org/10.3390/molecules28052209.

(21) Jasim' And, F.; Ali, F. *Measurements of Some Spectrophotometric Parameters of Curcumin in 12 Polar and Nonpolar Organic Solvents*; **1989**; Vol. 39.

(22) Hung, Y. C.; Jiang, J. C.; Chao, C. Y.; Su, W. F.; Lin, S. T. Theoretical Study on the Correlation between Band Gap, Bandwidth, and Oscillator Strength in Fluorene-Based Donor-Acceptor Conjugated Copolymers. *J. Phys. Chem. B* **2009**, *113* (24), 8268–8277. https://doi.org/10.1021/jp9018603.

(23) Villares, A.; Lydon, D. P.; Porrés, L.; Beeby, A.; Low, P. J.; Cea, P.; Royo, F. M. Preparation of Ordered Films Containing a Phenylene Ethynylene Oligomer by the Langmuir-Blodgett Technique. *J. Phys. Chem. B* **2007**, *111* (25), 7201–7209. https://doi.org/10.1021/jp072052h.

(24) Jurak, M.; Szafran, K.; Cea, P.; Martín, S. Analysis of Molecular Interactions between Components in Phospholipid-Immunosuppressant-Antioxidant Mixed Langmuir Films. *Langmuir* **2021**, *37* (18), 5601–5616. https://doi.org/10.1021/acs.langmuir.1c00434.

(25) Oliveira, O. N.; Udia Bonardi, C. *The Surface Potential of Langmuir Monolayers Revisited*; **1997**. https://pubs.acs.org/sharingguidelines.

(26) Subhan, M. A.; Alam, K.; Rahaman, M. S.; Rahman, M. A.; Awal, R. Synthesis and Characterization of Metal Complexes Containing Curcumin ($C_{21}H_{20}O_6$) and Study of Their Anti-Microbial Activities and DNA-Binding Properties. *J. Sci. Res.* **2013**, *6* (1), 97–109. https://doi.org/10.3329/jsr.v6i1.15381.

(27) Acikbas, Y.; Tetik, G. D.; Ozkaya, C.; Bozkurt, S.; capan, R.; Erdogan, M. Developing of N-(4-Methylpyrimidine-2-Yl)Methacrylamide Langmuir–Blodgett Thin Film Chemical Sensor via Quartz Crystal Microbalance Technique. *Microsc. Res. Tech.* **2020**, *83* (10), 1198–1207. https://doi.org/10.1002/jemt.23511.

(28) Mcrae, E. G.; Kasha, M. Enhancement of Phosphorescence Ability upon Aggregation of Dye Molecules [6]. *J. Chem. Phys.* **1958**, 721–722. https://doi.org/10.1063/1.1744225.

(29) Rubinger, C. P. L.; Moreira, R. L.; Cury, L. A.; Fontes, G. N.; Neves, B. R. A.; Meneguzzi, A.; Ferreira, C. A. Langmuir-Blodgett and Langmuir-Schaefer Films of Poly(5-Amino-1-Naphthol) Conjugated Polymer. *Appl. Surf. Sci.* **2006**, *253* (2), 543–548. https://doi.org/10.1016/j.apsusc.2005.12.096.